A Habenula Neural Biomarker Simultaneously Tracks Weekly and Daily Symptom Variations during Deep Brain Stimulation Therapy for Depression

Shi Liu[1,2,3,9], Yu Qi[1,3], Shaohua Hu[4], Ning Wei[4], Jianmin Zhang[5], Junming Zhu[5], Hemmings Wu[5], Hailan Hu[6], Yuxiao Yang[1,2,3,5,7*] and Yueming Wang[1,3,8*]

[1] *MOE Frontier Science Center for Brain Science and Brain-machine Integration, Nanhu Brain-computer Interface Institute, Hangzhou, 310058, China.*
[2] *State Key Laboratory of Brain-machine Intelligence, Hangzhou, 311100, China.*
[3] *College of Computer Science and Technology, Zhejiang University, Hangzhou, 310058, China.*
[4] *Department of Psychiatry, The First Affiliated Hospital, Zhejiang University School of Medicine, Hangzhou, 310003, China.*
[5] *Department of Neurosurgery, The Second Affiliated Hospital of Zhejiang University, Hangzhou, 310058, China.*
[6] *School of Brain Science and Brain Medicine, Zhejiang University, Hangzhou, 310058, China.*
[7] *NHC and CAMS Key Laboratory of Medical Neurobiology, Zhejiang University, Hangzhou, 310058, China.*
[8] *Qiushi Academy for Advanced Studies, Zhejiang University, Hangzhou, 310058, China.*
[9] *Lingang Laboratory, Shanghai, 200031, China.*
* *Corresponding author(s). E-mail(s): yuxiao.yang@zju.edu.cn; ymingwang@zju.edu.cn*

Running title: A Habenula Biomarker for Depression DBS Therapy

Keywords: deep brain stimulation; treatment-resistant depression; habenula; local field potential; neural biomarker; machine learning

Abstract

Deep brain stimulation (DBS) targeting the lateral habenula (LHb) is a promising therapy for treatment-resistant depression (TRD) but its clinical effect has been variable, which can be improved by adaptive DBS (aDBS) guided by a neural biomarker of depression symptoms. A clinically-viable neural biomarker is desired to classify depression symptom states, track both slow and fast symptom variations during the treatment, and respond to DBS parameter alterations, which is currently lacking. Here, we conducted a study on one TRD patient who achieved remission following a 41-week LHb DBS treatment, during which we assessed slow symptom variations using weekly clinical ratings and fast variations using daily self-reports. We recorded daily LHb local field potentials (LFP) concurrently with the reports during the entire treatment process. We then used machine learning methods to identify a personalized depression neural biomarker from spectral and temporal LFP features. The identified neural biomarker classified high and low depression symptom severity states with a cross-validated accuracy of 0.97. It further simultaneously tracked both weekly (slow) and daily (fast) depression symptom variation dynamics, achieving test data explained variance of 0.74 and 0.63, respectively. It finally responded to DBS frequency alterations. Our results hold promise to identify clinically-viable neural biomarkers to facilitate future aDBS for treating TRD.

1. Introduction

Major depressive disorder (MDD) is one of the most common neuropsychiatric disorders, affecting over 300 million individuals worldwide [1] . Approximately 30%

of MDD patients are treatment-resistant, meaning they do not respond adequately to at least two antidepressant trials [2]. Deep brain stimulation (DBS) is a neurosurgical procedure that allows targeted circuit-based neuromodulation [3]. It has emerged as a promising treatment option for patients with treatment-resistant depression (TRD) [4–6], as shown by open-label studies targeting various brain structures involved in the brain's "reward" system that mediates positive motivations. Such targets include the subcallosal cingulate cortex (SCC) [7], the ventral capsule/ventral striatum (VC/VS) [8], the medial forebrain bundle (MFB) [9], and the bed nucleus of the stria terminalis (BNST) [10]. However, several recent double-blinded clinical trials have shown that the effects of DBS targeting these brain structures are inconsistent across patients [11–15]. As a potential improvement over DBS, adaptive DBS (aDBS) optimizes DBS parameters in real-time by using neural signals as feedback for enhancing clinical efficacy [16]. A recent study implements aDBS targeting VC/VS in a TRD patient by triggering stimulation only when the local field potential (LFP) signal pattern indicates worsening of depression symptoms, achieving rapid alleviation of depression symptoms [17].

The lateral habenula (LHb) is a hub structure that plays a central role in the brain's "anti-reward" system that mediates negative motivations [18–20]. Animal studies have systematically shown that the local bursting firing patterns in LHb are closely related to depression-like behaviors and that neuromodulation of LHb has significant antidepressant effects [21,22]. Several clinical studies have reported single-patient depression symptom alleviation following LHb DBS since 2010 [23–26]. On the other hand, two recent clinical studies on seven or six patients has shown more variable effects of LHb DBS across patients [27,28] Similar to other DBS targets,

aDBS for LHb also provides a promising path towards improved and more consistent treatment effects across TRD patients.

A critical and fundamental requirement for developing LHb aDBS is the identification of an LHb neural biomarker of depression symptoms during the DBS treatment to provide the necessary feedback signal [29,30]. A population-level SCC LFP spectral power biomarker has been identified for tracking depression symptom recovery with SCC DBS in five TRD patients [31]. Personalized amygdala and BNST LFP gamma power biomarkers have been identified for optimizing VC/VS DBS [32]. For LHb DBS, LFP signals have been recorded before the DBS treatment starts but not during the multi-month-long treatment process [27,28,33] and several studies have found statistical correlations between pre-treatment LHb LFP spectral features and after-treatment depression symptom ratings [27,28,33]. However, it is unknown whether the identified LFP features can classify depression symptom severity states or track the temporal dynamics of depression symptom variations during the DBS treatment process. Therefore, a useful neural biomarker for realizing LHb aDBS is still lacking.

A clinically-viable neural biomarker is desired to be able to track both the slow and fast temporal dynamics of depression symptom variations during DBS. This is because both natural and DBS-induced depression symptom changes can vary at different time scales, with both slow-changing dynamics over months or weeks [34–38] and fast-changing dynamics over hours or days [9,39–42]. Existing neural biomarker studies have focused on tracking the temporal dynamics of either slow or fast symptom variations. The aforementioned SCC neural biomarker for SCC DBS tracks the temporal dynamics of the weekly symptom variations over 24 weeks [31].

The aforementioned amygdala and BNST neural biomarkers for VC/VS DBS track the faster temporal dynamics of symptom variations within several days [17,32]. Several other studies have also identified resting-state (without DBS) neural biomarkers of relatively fast depression symptom variations within several days using multisite intracranial electroencephalography (iEEG) [43–45]. However, to date, identifying a neural biomarker that can simultaneously track the temporal dynamics of both slow and fast depression symptom variations, in particular during LHb DBS treatment, remains elusive.

Moreover, the neural biomarker needs to reflect the dose effect of different DBS parameters for optimizing stimulation parameters in aDBS. Since the DBS mechanism for treating TRD is largely unknown [46], only few studies have experimentally explored the dose effect of different DBS amplitudes on human neural signals [17,31,32]. On the other hand, DBS frequency also has been shown to play a key role in altering TRD symptoms [4–6,47]. However, how different LHb DBS parameters, especially stimulation frequencies, alter neural signals or neural biomarkers in TRD patients remains unknown.

Here, to close the above gaps, we conducted LHb DBS on one TRD patient where we evaluated the patient's symptoms and concurrently collected daily LHb LFP signals during the entire 41-week long treatment process (Figure 1A). With this unique dataset and by using machine learning techniques, we identified a clinically-viable neural biomarker from spectral and temporal LHb features that (1) accurately classified high and low depression symptom severity states; (2) significantly tracked the temporal dynamics of weekly (slower) and daily (faster) depression symptom variations during the DBS treatment; (3) reflected the depression symptom changes

in response to DBS frequency alterations. Together, our results have implications for identifying clinically-viable neural biomarkers to facilitate future LHb aDBS developments for treating TRD.

2. Materials and Methods

2.1 Participant

This study included a male TRD patient aged 36-40 years old (see Note S1 for detailed patient medical information) participating in a clinical trial of LHb DBS treatment starting in October 2021. The patient provided informed consent for participation in the clinical trial. This study received approval from the Ethics Committee of Zhejiang University School of Medicine Second Affiliated Hospital (protocol number 20210218). It was registered at www.clinicaltrials.gov (NCT05716555), where detailed information regarding the inclusion and exclusion criteria can be accessed.

At the beginning of the clinical trial, two independent psychiatrists evaluated the patient's psychotic symptoms using the 17-item Hamilton Depression Rating Scale (HAMD), the Montgomery Asberg Depression Scale (MADRS), and the Hamilton Anxiety Rating Scale (HAMA) as baseline assessments. In addition to the psychiatric assessments, the patient underwent a comprehensive physical examination, various mental scale assessments, and a magnetic resonance imaging (MRI) examination. We carefully ensured that other psychiatric diagnoses outlined in the Diagnostic and Statistical Manual of Mental Disorders-Fifth Edition (DSM-5) were excluded.

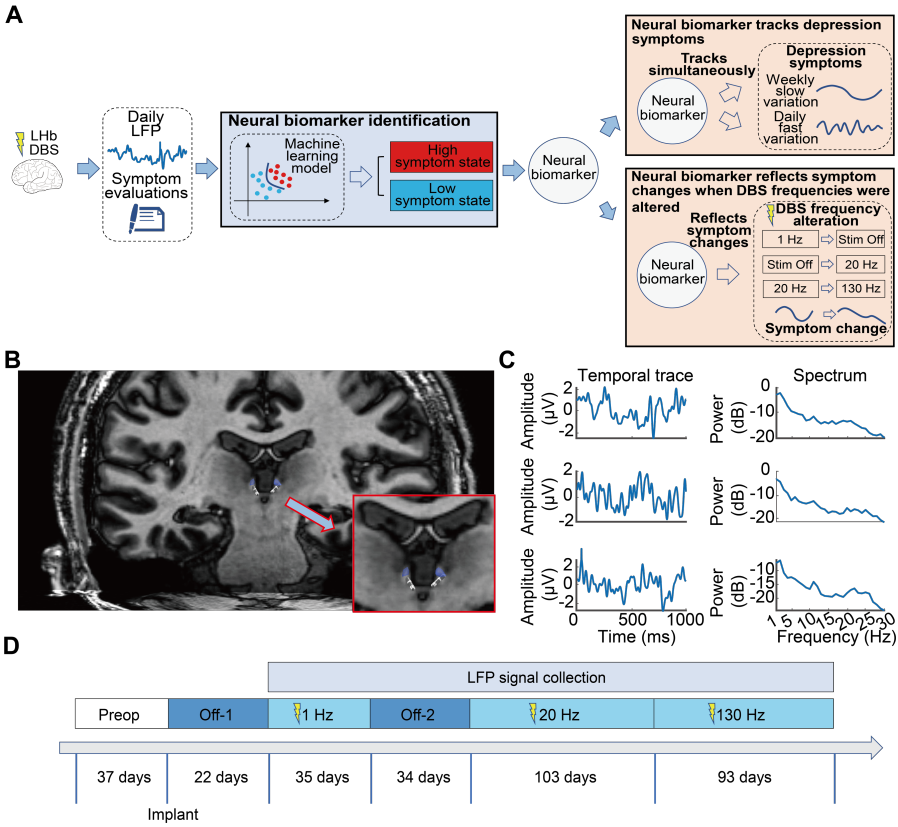

Figure 1. Study framework and experiment design. (A) During the LHb DBS treatment of one TRD patient, we used weekly clinical ratings and daily self-reports to evaluate the symptom variations, where we simultaneously collected daily LFP signals from LHb. Using machine learning models, we identified a neural biomarker that classified high and low depression symptom states during the DBS treatment. Using data not used in neural biomarker identification, we evaluated the neural biomarker in terms of 1) simultaneously tracking the temporal dynamics of weekly slow and daily fast variations of depression symptoms; 2) reflecting symptom changes when DBS frequencies were altered. (B) MRI visualization showing the DBS lead placement within the patient's LHb. The shaded blue area indicates the volume of tissue activated (VTA) by the DBS. (C) Temporal dynamics and spectrum of example epochs of LFP signals after preprocessing. (D) LHb DBS Treatment Timeline. The entire treatment process consisted of six stages. LFP signal collection began after the activation of 1 Hz stimulation.

2.2 Surgical procedure

A standard DBS implantation procedure was employed. Bilateral quadripolar electrodes (1200-40, SceneRay, Suzhou, China) were surgically implanted in the LHb

under local anesthesia (Figure 1B). The DBS electrodes had a diameter of 1.27 mm and a lead length of 400 mm. Each electrode's four contacts measured 1.5 mm in length with a spacing of 0.5 mm. The LHb targeting was guided by preoperative MRI sequences. After confirming the absence of stimulation side effects through intraoperative testing, an implantable pulse generator (SR1101, SceneRay) was placed under general anesthesia. The DBS device was also capable of recording and wireless transmitting LFP signals (Figure 1C).

2.3 DBS treatment process and symptom evaluations

During the bilateral DBS treatment process, we made multiple adjustments to the stimulation parameters to achieve the best therapeutic effect. We divided the treatment process into six stages based on the alterations of stimulation parameters (Figure 1D): 1) the "Preop" stage, the time before the DBS electrode implantation; 2) the "Off-1" stage, patient recovery with DBS turned off; 3) the "1 Hz" stage, activation of 1 Hz stimulation; 4) the "Off-2" stage, DBS turned off because of unnoticed power off; 5) the "20 Hz" stage, re-activation of 20 Hz stimulation; 6) the "130 Hz" stage, activation of 130 Hz stimulation. More details can be found in Note S2. The entire duration of DBS treatment spanned 41 weeks (starting from DBS electrode implantation).

The efficacy of DBS treatment was evaluated from two perspectives: clinician evaluation and self evaluation. For clinician evaluation, a psychologist blinded to the current stimulation parameters and their adjustments evaluated the patient's depression and anxiety symptoms on a weekly basis using standardized rating scales (HAMD, MADRS, HAMA). Response is defined as a 50% or greater improvement

on the HAMD score from the pre-treatment baseline. Remission is defined as achieving a HAMD score of 7 or less. The psychologist also evaluated the patient's emotional blunting and cognitive functioning during the treatment (see Note S3). For self evaluation, the patient used the Visual Analogue Scale (VAS) for depression (VAS-D) and anxiety (VAS-A) to self-report the symptom severity. Self-reported VASA and VAS-D had been used to assess the rapid effects of antidepressants [48]. To facilitate daily data collection, we established an online questionnaire system where the patient could conveniently complete the self-reports via the smartphone or computer.

2.4 LFP signal recording, signal processing, and feature extraction

After activating the 1 Hz stimulation, we collected daily LFP signals (30 minutes per day) concurrent with daily self-reported VAS-D and VAS-A (details in section 2.3). LFP signals were recorded at a sampling rate of 1000 Hz. Notably, stimulation was deactivated during the signal acquisition process. We reconstructed the electrode positions using MRI and selected two contacts in the left hemisphere for bipolar recording of a single LFP channel. The patient was instructed to attempt daily LFP recording and VAS-D/VAS-A reporting. Throughout the entire 41-week (287-day) treatment, the patient was able to activate LFP recording and report VAS-D and VAS-A on 122 days distributed across 26 weeks. Therefore, the subsequent analyses focused on the LFP signals, VAS-D, and VAS-A scores recorded from these 122 days, and the HAMD, MADRS, and HAMA scores recorded for the 26 weeks.

Custom MATLAB scripts (MathWorks Inc., Natick, MA, USA) were used to preprocess the LFP signals. The LFP signals were first band-pass filtered from 1 to 30 Hz using a Butterworth filter of order 12 to avoid the noise observed in higher frequency bands. Then, we divided the daily 30-minute LFP signals into 10-second epochs with a 50% overlap. Next, we used a standard procedure (details in Note S4) to remove bad epochs from daily LFP signals (example temporal traces and spectrum of preprocessed LFP epochs were shown in Figure 1C).

For each remaining LFP epoch, we computed its spectral domain (SD) and temporal domain (TD) features. SD features included PSD of the four bands (δ (1-4 Hz), θ (4-8 Hz), α (8-12 Hz), and β (12-30 Hz)) and phase-amplitude coupling (PAC) for six specific pairs of coupling. TD features included fourteen temporal domain features used in previous study [49], e.g., Hjorth mobility, singular value decomposition (SVD) Fisher information, Hurst exponent, etc. These features capture the temporal properties of LFP from probabilistic distribution and information theory perspectives and have been widely used in brain signal analyses [50,51]. As a result, we obtained 24 features, comprising 10 SD features and 14 TD features for each LFP epoch. Details of these 24 features are included in Table S1 and Note S4. Finally, we averaged each feature across LFP epochs within the same day and obtained a single averaged 24-dimensional LFP feature vector. Our subsequent analyses were based on the daily LFP features as computed above.

2.5 Identification of neural biomarker

We first conducted Spearman's rank correlation analyses between LFP features and symptoms. For each day, we correlated each daily LFP feature with the daily VAS-D

and VAS-A self-reports. For each week, we computed the average of LFP features across the days that belonged to this week, resulting in weekly LFP features; we then correlated each weekly LFP feature with the weekly clinical evaluation scales HAMD, HAMA, and MADRS. Bonferroni correction was used to adjust for multiple comparisons.

Next, we used a data-driven method to identify an LHb neural biomarker of depression symptoms, where we built a machine learning model to use LFP features to classify high and low depression symptom states.

First, we defined the high and low depression symptom states of the patient by k-means clustering the weekly depression scales HAMD and MADRS similar to prior work [17]. Among the total 26 weeks (122 days) of LFP data, 7 weeks (29 days) of LFP data belonged to the low depression symptom state (labeled 0), 4 weeks (22 days) of LFP data belonged to the high depression symptom state (labeled 1). The remaining 15 weeks (71 days) were unlabeled and used as test data for subsequent biomarker tracking evaluation (see next section).

Second, based on the labeled data, we built a machine learning model to use the LFP features to classify high and low depression symptom states. We constructed six machine learning models: logistic regression (LR), multilayer perceptron (MLP), adaptive boosting (AdaBoost), support vector machine (SVM), random forest (RF), and linear discriminant analysis (LDA). We trained and tested these models using 5-fold cross-validations that were repeated 200 times, where we computed the averaged cross-validated classification accuracy, specificity, sensitivity, F1 score, and Receiver Operating Characteristic (ROC) Area Under the Curve (AUC) score as the

performance metrics. The model with the highest accuracy was selected for further analysis.

Third, the chosen model was retrained with all labeled data, leading to a "neural biomarker model". This model takes the LFP feature as input and outputs the decision variable as the neural biomarker value (e.g., in the LR model, the decision variable was computed from the decision probability via the inverse sigmoid function). This allows us to compute a neural biomarker value for any given LFP feature. Higher neural biomarker values indicate more severe depression symptoms.

In essence, our identified neural biomarker aggregates spectral and temporal domain features from the LHb LFP signal to classify high and low depression states during DBS treatment.

2.6 Evaluation of the neural biomarker

We evaluated the identified neural biomarker in terms of (1) tracking the temporal dynamics of weekly symptom variations; (2) tracking the temporal dynamics of daily symptom variations; (3) reflecting changes in symptom variations induced by DBS frequency alterations.

First, we investigated tracking the temporal dynamics of weekly depression and anxiety symptom scales that were not used in neural biomarker identification. We took the daily LFP features as inputs to the neural biomarker model and computed the output daily neural biomarkers. We then averaged the daily neural biomarkers belonging to the same week to compute the weekly neural biomarkers. We next correlated the weekly neural biomarker values with the weekly HAMD, MADRS, and HAMA scores, respectively, using Spearman's rank correlation analysis with

explained variance (EV) as an estimation. We further analyzed the temporal dynamics in the neural biomarker and symptoms, using the dynamic time warping (DTW) distance [52] to measure the temporal tracking ability of the neural biomarker. Both the neural biomarker values and the symptom scales were normalized to a range of 0 to 1. We used a size three Sakoe–Chiba warping window in the DTW analysis following prior work [17,53]. A smaller DTW distance represents better temporal tracking. To determine the significance of the computed DTW distance, we randomly shuffled the temporal sequence of the neural biomarker 10,000 times and used the corresponding shuffled DTW distances as the null hypothesis distribution for computing the *P* value.

Second, we investigated tracking the temporal dynamics of the daily VAS-D and VAS-A self-reports, which were also not used in neural biomarker identification. Similar to the weekly case, daily LFP features were used to generate daily neural biomarkers, which were then correlated with daily VAS-D and VAS-A reports. DTW was again used to assess the temporal tracking of daily depression symptom variations.

Third, we qualitatively compared trends in weekly neural biomarkers and depression ratings across three DBS frequency alterations (1 Hz to Off-2, Off-2 to 20 Hz, 20 Hz to 130 Hz). We used the two-sided Wilcoxon rank-sum test to check whether there was a significant difference between the two stages before and after alteration. We also averaged the neural biomarker values and depression ratings across five time periods for each case: 1) from the beginning of this stage to two weeks before the alteration week; 2) during the week before the alteration week; 3) during the alteration week; 4) during one week after the alteration week; 5) averaged from two weeks after the alteration week to the end of this stage.

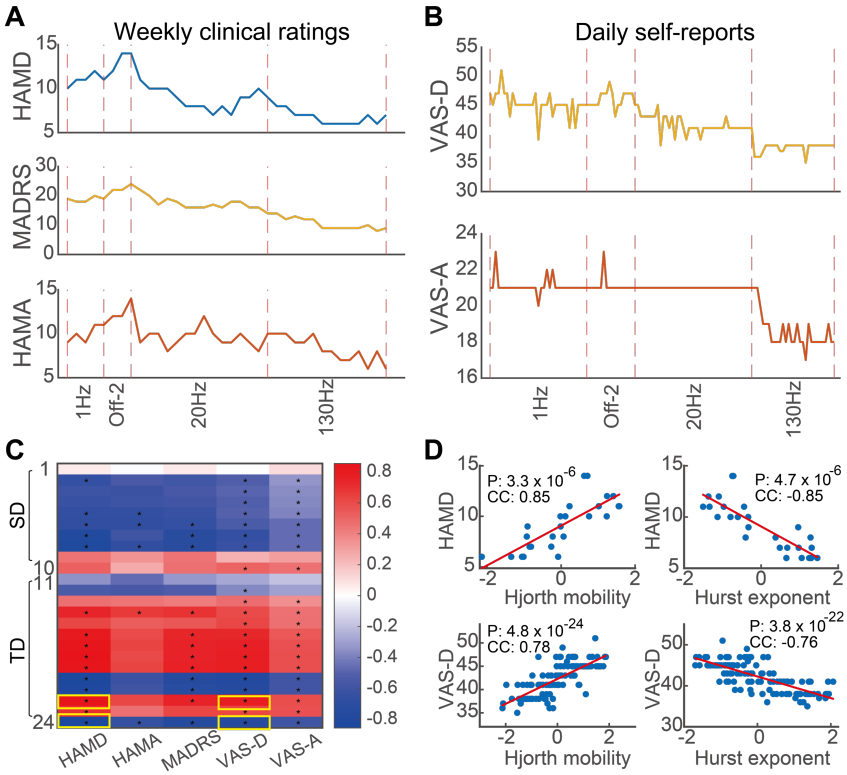

Figure 2. Changes of weekly and daily symptom scores during the LHb DBS treatment and their correlations with LFP temporal and spectral domain features. (A) Changes of weekly clinical ratings during the treatment. The vertical dashed lines represent different treatment stages indicated by the x-axis labels. (B) Changes of daily self-reports during the treatment. The vertical dashed lines represent different treatment stages indicated by the x-axis labels. (C) Heatmap of the correlation coefficients. Each cell shows the correlation coefficient (CC) value between one LFP feature (y-axis) and one symptom score (x-axis), and cells marked with * indicate the coefficients that are significantly different from zero (Bonferroni corrected $p<0.05$). (D) Positive and negative correlation examples with the weekly HAMD score and daily VAS-D score as shown by the yellow boxes in (C).

3. Results

3.1 LHb DBS improved the patient's clinical symptoms, which were significantly correlated with LHb LFP features

We first examined the TRD patient's symptom changes throughout the LHb DBS treatment process. At the beginning of treatment, the patient's baseline HAMD score

was 20, MADRS score was 25, and HAMA score was 16. In terms of the weekly clinical ratings (Figure 2A), the patient responded at week 14 (HAMD score dropped to 10; MADRS score dropped to 19; HAMA score dropped to 8) and achieved remission by the end of the 41-week treatment (HAMD score was 7; MADRS score was 9; HAMA score was 6). The daily self-reports followed a similar decreasing trend (Figure 2B). Such a consistent trend was confirmed by the strong positive correlation between the daily self-reports and weekly clinical ratings (Spearman's $\rho > 0.5$, $P < 0.05$ for all pair-wise correlations; see Table S2 and Figure S1 for details). Besides alleviating the symptoms based on the weekly clinical ratings and daily self-reports, we also found improvement in emotional blunting and cognitive functioning (Note S3 and Tables S3-S5).

During the LHb DBS treatment process, we recorded daily LHb LFP signals. Therefore, we investigated how the LFP features correlated with the patient's symptom changes. We found that many of the temporal and spectral domain LHb LFP features were significantly correlated with the weekly clinical ratings and daily self-reports (Figure 2C). For example, Hurst exponent exhibited the strong correlations with both weekly HAMD scores (Figure 2D, Spearman's $\rho = -0.85$, Bonferroni corrected $P = 4.7 \times 10^{-6}$) and daily VAS-D scores (Figure 2D, Spearman's $\rho = -0.76$, Bonferroni corrected $P = 3.8 \times 10^{-22}$). These results show that LHb LFP temporal and spectral domain features were strongly correlated with weekly and daily depression symptom scores, indicating that it is feasible to identify an LHb neural biomarker of depression symptoms from the LFP temporal and spectral domain features.

3.2 Accurate classification of high and low depression symptom severity states led to the identification of an LHb neural biomarker

We next used the LFP temporal and spectral features to identify a neural biomarker that can classify high and low depression symptom severity states. We started by defining a state of high symptom severity and a state of low symptom severity via clustering the weekly depression scales HAMD and MADRS (Figure 3A). The high symptom state (7 weeks) had an average HAMD score of 12.8 and an average MADRS score of 22.5, while the low symptom state (4 weeks) had an average HAMD score of 6.3 and an average MADRS score of 9.0. We then used LFP temporal domain and spectral domain features from these 11 weeks to classify the high and low symptom severity states via six machine learning models in cross-validation. Among these six models, the LR model performed better than other more complicated models (Figure 3B and table S6). Specifically, for the LR model, the cross-validated classification accuracy was 0.973 ± 0.002 (Mean $\pm$ SEM), the specificity was 0.961 ± 0.003, the sensitivity was 0.988 ± 0.002, the F1-score was 0.970 ± 0.002, and the AUC score was 0.974 ± 0.001, which were all significantly higher than other models (Wilcoxon rank sum test, Bonferroni corrected $P < 0.05$ for all comparisons), suggesting that the LR model was best suited for classifying the collected data. We thus selected the LR model for further analysis. Then, we retrained the LR model using all labeled data, resulting in the neural biomarker model. The neural biomarker model takes the LFP features as input and outputs the model

decision value as the identified neural biomarker, with higher values indicating worse depression symptoms.

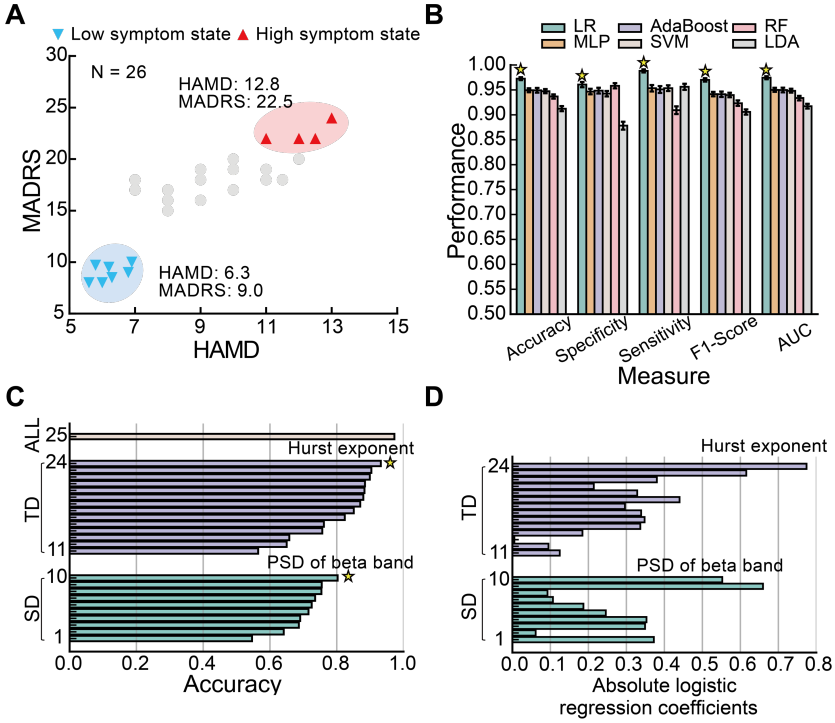

Figure 3. Accurate classification of high and low depression symptom severity states by the identified neural biomarker. (A) Clustering of depression symptom severity states. We clustered the HAMD and MADRS scores to obtain two distinct symptom states: a high depression symptom severity state (shaded in red) and a low depression symptom severity state (shaded in blue). Each point represents data of a week. The average HAMD and MADRS scores of the two clusters are also indicated in the figure. (B) Classification performance of different classifiers. The bar represents mean and the whiskers represent the 95% confidence interval. Six classification models (different colors) were compared in terms of five performance matrices (different x-axis groups): accuracy, specificity, sensitivity, F1-Score and AUC. The best model was indicated by a yellow star for each metric. Classification model names and abbreviations: logistic regression (LR), multilayer perceptron (MLP), adaptive boosting (AdaBoost), support vector machine (SVM), random forest (RF), and linear discriminant analysis (LDA). (C) Classification accuracy of individual features and all LFP features by the logistic regression model. The individual SD features are in green, and their indices are ordered based on classification accuracy. The individual TD features are in blue, and their indices are ordered by classification accuracy. The combination of all LFP features is in brown. The best individual feature was indicated by a yellow star for each domain. (D) The absolute coefficients of each feature in the logistic regression model trained with all LFP features. The individual feature indices are the same as in (C).

We further investigated how different features contributed to identifying the neural biomarker by performing separate classifications for each feature (Figure 3C). The best temporal domain feature was the Hurst exponent, with a cross-validated classification accuracy of 0.932. While the best spectral domain feature was the PSD of the β band, with an average accuracy of 0.803. Overall, temporal domain features (average accuracy: 0.781) outperformed spectral domain features (average accuracy: 0.705). Notably, combining all the LFP features yielded superior performance compared to individual features. Consistently, by investigating the logistic regression coefficients of the neural biomarker model (Figure 3D), we found that the features with better classification accuracy also had larger coefficients in the neural biomarker model. These results show that the temporal domain and spectral domain features had supplementary information that both contributed to the identification of the neural biomarker, with temporal features having a stronger influence.

3.3 The identified neural biomarker simultaneously tracked the temporal dynamics of weekly and daily depression symptom variations during LHb DBS treatment

After identifying the neural biomarker of depression symptoms, we evaluated its ability to track the temporal dynamics of slow (weekly) and fast (daily) depression symptom variations during the LHb DBS treatment. For slow weekly variations, we used the identified neural biomarker model to compute weekly neural biomarker values (see Methods section 2.6 for details). We used the weekly neural biomarker values to predict the associated weekly clinical ratings, where we strictly excluded the weekly data that were used to identify the neural biomarker (i.e., the prediction

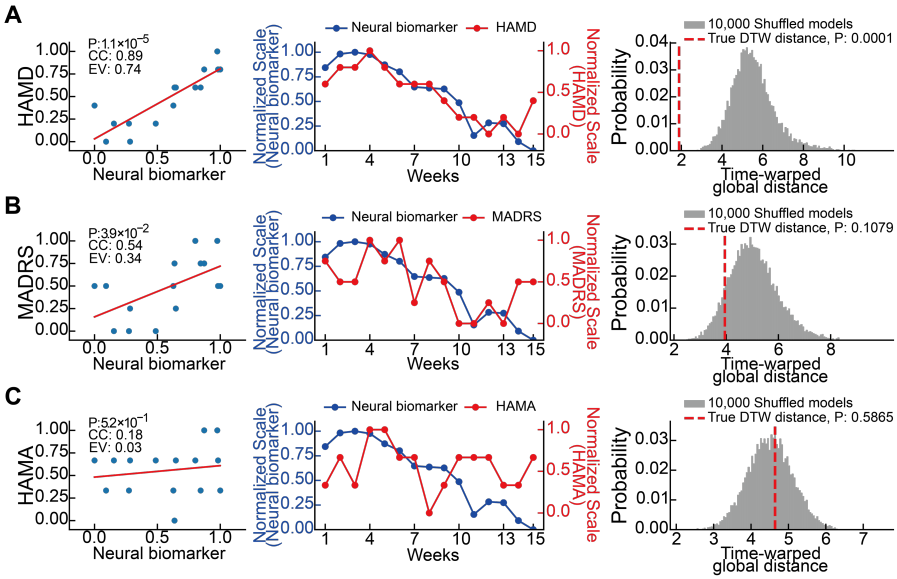

Figure 4. Accurate tracking the temporal dynamics of weekly depression symptom variations by the identified neural biomarker. (A) Left: correlation between the identified neural biomarker values and the weekly HAMD scores unseen in neural biomarker identification. EV: Explained variance. Middle: neural biomarker tracking of the weekly HAMD score dynamics over time. Right: the DTW distance analysis result for evaluating the significance of tracking in the middle panel. Smaller DTW distance represents better tracking. Note that we normalized both the neural biomarker values and the symptom scales to a range of 0 to 1 using min-max normalization for better visualization. (B) same as (A) but for the weekly MADRS scores. (C) same as (A) but for the weekly HAMA scores.

was based on new unseen data not used in training the neural biomarker model). We found that the weekly neural biomarker values significantly predicted the HAMD scores (Figure 4A, EV=0.74, $P = 1.1 \times 10^{-5}$). Further, considering the temporal dynamics in detail by using the DTW distance analysis (see Methods section 2.6), we found that the weekly neural biomarker significantly tracked the temporal dynamics of weekly HAMD score variations (random shuffle $P = 0.00001$). Consistently, the weekly neural biomarker values significantly predicted the MADRS scores (Figure 4B, EV=0.34, $P = 0.039$), and tracked the temporal dynamics in the DTW distance analysis with marginally significant statistics (random shuffle $P = 0.1079$). Converse-

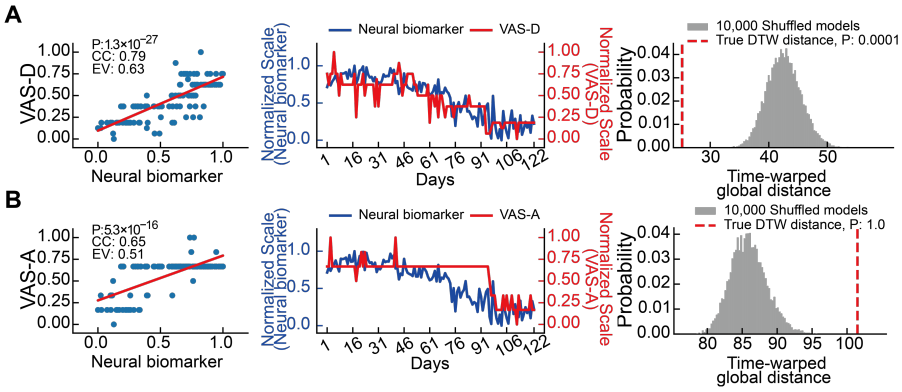

Figure 5. Accurate tracking the temporal dynamics of daily depression symptom variations by the identified neural biomarker. (A) Left: correlation between the identified neural biomarker values and the daily VAS-D scores unseen in neural biomarker identification. EV: Explained variance. Middle: neural biomarker tracking of the daily VAS-D score dynamics over time. Right: the DTW distance analysis result for evaluating the significance of tracking in the middle panel. Smaller DTW distance represents better tracking. (B) same as (A) but for the daily VAS-A scores.

ly, the weekly neural biomarker values did not predict the HAMA scores (Figure 4C, EV=0.03, $P = 5.2 \times 10^{-1}$) or tracked the temporal dynamics (random shuffle P = 0.5865).

For fast daily variations, we used the identified neural biomarker model to compute daily neural biomarker values and used the daily neural biomarker values to predict the associated daily self-reports (again, data not used in training the neural biomarker model). We found that the daily neural biomarker values significantly predicted the VAS-D scores (Figure 5A, EV=0.63, $P = 1.3 \times 10^{-27}$) and showed significant tracking of VAS-D dynamics (random shuffle P = 0.0001). By contrast, while the daily neural biomarker values predicted the VAS-A scores (Figure 5B, EV=0.51, $P = 5.3 \times 10^{-16}$) but the daily neural biomarker did not track VAS-A dynamics (random shuffle P = 1.00).

In summary, the results show that the identified neural biomarker significantly tracked the temporal dynamics of both weekly and daily variations in depression

448 symptoms during the LHb DBS treatment and specifically tracked depression
449 symptoms rather than anxiety symptoms.

450 3.4 The identified neural biomarker reflected changes of 451 depression symptoms in response to DBS parameter 452 alterations

453 A useful neural biomarker for DBS also needs to reflect the effect of different DBS
454 parameters. We thus finally evaluated if the identified neural biomarker could reflect
455 changes in depression symptoms in response to DBS parameter alterations. We
456 applied three different DBS frequencies during the treatment: 1 Hz, 20 Hz, and 130
457 Hz. For the DBS alteration from 1 Hz to stimulation off (Off-2, the DBS device shut
458 down due to unnoticed power off), there was a trend of increasing for the neural
459 biomarker, HAMD, and MADRS while the statistical tests were not significant due
460 the limited sample size (Figure 6A, 1Hz v.s. stimulation off, normalized mean±s.e.m.,
461 neural biomarker: 0.912 ± 0.055 v.s. 0.956 ± 0.026, P=0.35; HAMD: 0.562 ± 0.062
462 v.s. 0.688 ± 0.036, P=0.16; MADRS: 0.656 ± 0.031 v.s. 0.734 ± 0.053, P=0.35),
463 which indicated a rebound trend of depression symptoms due to the disruption of DBS
464 treatment. For the DBS alteration from stimulation off (Off-2) to 20 Hz stimulation
465 (Figure 6B), the neural biomarker, HAMD, and MADRS consistently decreased
466 (Figure 6B, stimulation off v.s. 20 Hz, neural biomarker: 0.905 ± 0.095 v.s. 0.545 ±
467 0.059, P=0.04; HAMD: 0.875 ± 0.125 v.s. 0.375 ± 0.072, P=0.05; MADRS: 0.875
468 ± 0.000 v.s. 0.606 ± 0.061, P=0.08). Specifically, the neural biomarker, HAMD and
469 MADRS scores all decreased at the week of DBS frequency alteration, further
470 decreased one week after the alteration and continued to decrease with more obvious

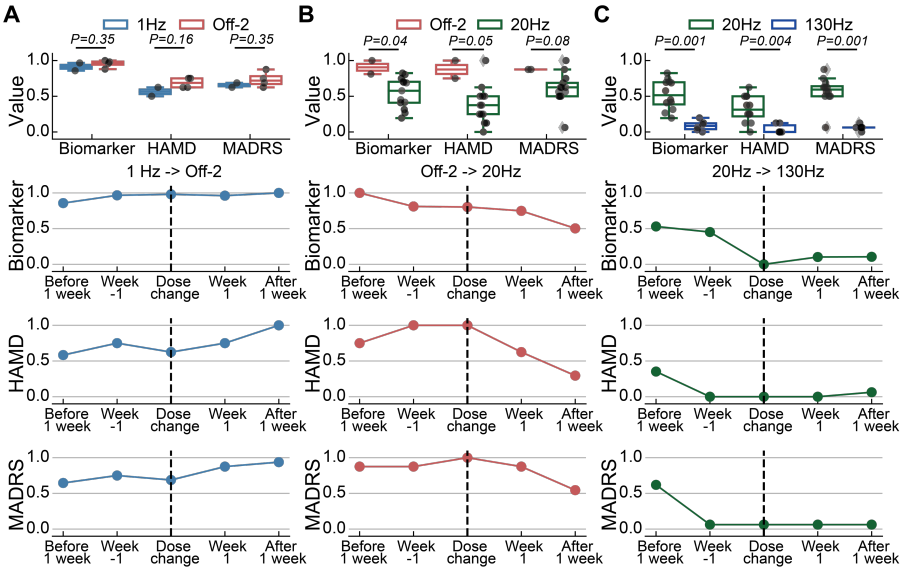

Figure 6. The consistent trend between the neural biomarker and the depression symptom changes when DBS frequencies were altered. (A) DBS frequency was altered from 1 Hz to Off-2. Top: comparison of the values of the biomarker, HAMD scores and MADRS scores between the 1Hz stage and Off-2 stage. Two-sided Wilcoxon rank-sum test was used for significance test. Row two: changes in the identified neural biomarker time-locked to the DBS frequency alteration week (vertical dashed line). Row three: changes in HAMD time-locked to the DBS frequency alteration week. Bottom: changes in MADRS time-locked to the DBS frequency alteration week. (B) same as (A) but for DBS frequency alteration from Off-2 to 20 Hz. (C) same as (A) but for DBS frequency alteration from 20 Hz to 130 Hz.

changes after week two. For the DBS alteration from 20 Hz to 130 Hz stimulation (Figure 6C), the neural biomarker, HAMD, and MADRS also consistently decreased (Figure 6C, 20 Hz v.s. 130 Hz, neural biomarker: 0.524 ± 0.060 v.s. 0.088 ± 0.029, P=0.001; HAMD: 0.323 ± 0.054 v.s. 0.042 ± 0.026, P=0.004; MADRS: 0.573 ± 0.056 v.s. 0.062 ± 0.016, P=0.001). More specifically, the neural biomarker, HAMD and MADRS scores already showed a trend of decreasing before the DBS frequency alteration, and the alleviated symptoms stayed relatively stable during the alteration week, at week one after the alteration, and the same stable trend continued after week two. The results suggested that the 1 Hz DBS did not induce an obvious change in depression symptoms, while the 20 Hz and 130 Hz DBS had more meaningful effects.

The results further demonstrated that the identified neural biomarker indeed reflected the different change patterns in depression symptoms when the DBS frequencies were altered.

4. Discussion

4.1 A data-driven LHb neural biomarker for tracking slow and fast depression symptom variations during DBS treatment

A mechanism-driven neural biomarker for depression is currently lacking mainly because the neural circuitry underlying depression has not been clearly delineated [54]. Therefore, current neural biomarkers of depression symptoms for tracking DBS effects have largely used data-driven machine learning methods to map LFP features to depression symptom ratings [17,31,32]. The usefulness of data-driven neural biomarkers critically depends on the data used to identify the neural biomarker. For example, a recent work [31] focused on a cingulate neural biomarker that was trained with and accordingly predicted longer-term (on the time scale of weeks) clinical ratings. On the other hand, another recent work [17] only trained and tested a neural biomarker with shorter-term (on the time scale of minutes) self-reports. Our work is unique in that while we identified our LHb neural biomarker based on weekly clinical ratings, we demonstrated that the neural biomarker predicted not only weekly clinical ratings (data not used in identification) but also daily self-reports (data again not used in identification). The results suggested that our LHb neural biomarker could track the temporal dynamics of both slow and fast depression symptom variations, which was useful for developing new aDBS strategies that are robust across different time

scales. It is worth noting that our LHb neural biomarker specifically tracked the temporal dynamics of weekly and daily depression symptom scores but not the anxiety symptom scores. It suggests that despite the overlapping of depression-related and anxiety-related brain networks [55], LHb neural activity is mainly related to depression, which is supported by prior animal studies [21,22].

Both population-level and personalized neural biomarkers of depression symptoms have been identified for tracking DBS effects. Population-level neural biomarkers are derived from data collected from several patients and have the benefits of being directly applicable to a new patient and robust interpretability of the neural biomarker's biophysical mechanism across patients [31]. By contrast, personalized neural biomarkers are derived from data collected from an individual patient, which is more powerful in capturing the unique characteristics of depression symptoms in each patient, especially given the large inter-individual variability in depression-related brain networks [56]. With the emerging capability of recording more data within a single patient using mobile devices, personalized neural biomarker models can be more accurate in tracking the temporal dynamics of depression symptom variations. With such trends, a personalized neural biomarker has been identified and used for realizing aDBS targeting VC/VS [17]. Our study identified a personalized neural biomarker that achieved accurate classification and tracking of depression symptom variations during the DBS treatment targeting LHb, confirming the usefulness of personalization. Nevertheless, population-level and personalized neural biomarkers can complement each other. For example, one can leverage a large amount of population data to train an interpretable population-level neural biomarker model,

followed by fine-tuning with personalized data to further improve its accuracy, which is an important future research direction.

4.2 Importance of fusing LFP temporal domain and spectral domain features to identify the neural biomarker

Previous studies have exclusively used LFP spectral domain features to identify the neural biomarker for depression [17,31,32]. By contrast, we found that both the LFP temporal domain and spectral domain features contributed to our neural biomarker and that the temporal domain features contributed relatively more than the spectral domain features. The main contributing temporal domain feature was the Hurst exponent. The Hurst exponent measures "long-term memory" in temporal dynamics and is associated with the autocorrelation of a time series [57]. Our results suggest that the LHb LFP signal's auto-correlations might change during DBS. The main contributing (top 2) spectral domain feature was the PSD of the β band. The LHb β band oscillation was also found to correlate with depression symptoms before DBS treatment in a previous study [27]. These findings highlight the significance of the β band oscillations in LHb as related to depression. Both the Hurst exponent and the β band oscillation features reflect the abnormal synchronization of LHb neural ensembles underlying depression and might be related to the abnormal burst spiking phenomena of LHb neurons found in rodents exhibiting depression-like behaviors [21,22]. The mechanism underlying the contributing LFP temporal domain and spectral domain features requires further investigation by future research.

4.3 DBS frequency deferentially modulates the depression symptom and neural biomarker

Prior studies have shown that DBS frequency can significantly influence the treatment efficacy for TRD, e.g., high-frequency DBS has generally yielded better treatment outcomes than low-frequency DBS [23,58,59]. Consistently, we discovered that a very low DBS frequency of 1 Hz was not effective in alleviating the depression symptoms in our patient, but higher frequencies of 20 Hz and 130 Hz were more effective. Beyond the depression symptom ratings, we additionally found that the neural biomarker was also consistently modulated by the different DBS frequencies. DBS frequency might influence the release of neurotransmitters in depression-targeted pathways [60], thus modulating the neural biomarker and the depression symptoms. However, similar to other DBS targets, the optimal DBS frequency at LHb is still also an open question that requires further research.

5. Limitations

Our study has several limitations. First, our study had a limited sample size (n-of-1); further studies with more patients are needed to confirm our findings on LHb neural biomarkers. Second, despite its powerful classification and tracking performance, our neural biomarker was identified using only one channel of LFP signals. Incorporating multi-channel LFP signals in future studies would allow for finding neural biomarkers with even better performance and a more comprehensive understanding of the neural mechanism underlying neural biomarker identification. Third, due to the high-frequency recording noise of our DBS device, we filtered the LFP signal below 30 Hz to ensure noise rejection. Future work with better recording capability should

investigate how higher-frequency LFP temporal and spectral domain features contribute to the identification of neural biomarkers. Finally, our LFP signals were recorded with the stimulation temporarily turned OFF to eliminate stimulation artifacts. While this approach ensured clean LFP signals, it is important to consider using LFP signals during stimulation to identify neural biomarkers, but this requires high-performance stimulation artifact removal, which remains challenging [61].

6. Conclusion

One patient with TRD reached remission after 41 weeks of LHb DBS treatment. With a unique data collection of concurrent daily and weekly depression symptom scores and LHb LFP signals during the entire treatment process, we used machine learning to identify an LHb neural biomarker of depression symptoms. We demonstrated that our LHb neural biomarker accurately classified high and low depression symptom severity states, simultaneously tracked the temporal dynamics of weekly (slow) and daily (fast) depression symptom variations during the DBS treatment process, and reflected the depression symptom changes in response to DBS frequency alterations. Our methods and results hold promise in identifying clinically-viable neural biomarkers to facilitate future adaptive DBS developments for treating TRD.

Data availability

The data supporting this study's findings are available from the corresponding author upon reasonable request.

Funding

This work was supported in part by the National Natural Science Foundation of China under Grants 62336007 and 62306269, in part by the Zhejiang Provincial Natural Science Foundation of China under Grant LD24H090001, in part by the Key R&D Program of Zhejiang under Grant 2022C03011, in part by the Starry Night Science Fund of Zhejiang University Shanghai Institute for Advanced Study under Grant SN-ZJU-SIAS-002, in part by the Non-profit Central Research Institute Fund of Chinese Academy of Medical Sciences under Grant 2023-PT310-01, and in part by the Fundamental Research Funds for the Central Universities under Grant 226-2024-00127.

Author Contributions

Shi Liu: Methodology, Software, Formal analysis, Writing - Original Draft, Visualization. Yu Qi: Investigation, Resources. Shaohua Hu: Conceptualization, Resources. Ning Wei: Resources, Data Curation, Writing - Original Draft. Jianmin Zhang: Conceptualization, Resources. Junming Zhu: Conceptualization, Resources. Hemmings Wu: Conceptualization, Investigation. Hailan Hu: Conceptualization. Yuxiao Yang: Conceptualization, Supervision, Methodology, Writing - Review & Editing, Funding acquisition. Yueming Wang: Conceptualization, Supervision, Project administration, Funding acquisition, Writing - Review & Editing. All authors revised and approved the final version of the manuscript.

Conflict of Interest

There are no financial conflicts of interest to disclose.

References

[1] Organization WH, others. Depression and other common mental disorders: global health estimates. World Health Organization; 2017.

[2] Otte C, Gold SM, Penninx BW, Pariante CM, Etkin A, Fava M, et al. Major depressive disorder. Nat Rev Dis Primer 2016;2:16065. https://doi.org/10.1038/nrdp.2016.65.

[3] Krauss JK, Lipsman N, Aziz T, Boutet A, Brown P, Chang JW, et al. Technology of deep brain stimulation: current status and future directions. Nat Rev Neurol 2021;17:75–87. https://doi.org/10.1038/s41582-020-00426-z.

[4] Dandekar MP, Fenoy AJ, Carvalho AF, Soares JC, Quevedo J. Deep brain stimulation for treatment-resistant depression: an integrative review of preclinical and clinical findings and translational implications. Mol Psychiatry 2018;23:1094–112. https://doi.org/10.1038/mp.2018.2.

[5] Figee M, Riva-Posse P, Choi KS, Bederson L, Mayberg HS, Kopell BH. Deep Brain Stimulation for Depression. Neurotherapeutics 2022;19:1229–45. https://doi.org/10.1007/s13311-022-01270-3.

[6] Johnson KA, Okun MS, Scangos KW, Mayberg HS, de Hemptinne C. Deep brain stimulation for refractory major depressive disorder: a comprehensive review. Mol Psychiatry 2024:1–13. https://doi.org/10.1038/s41380-023-02394-4.

[7] Mayberg HS, Lozano AM, Voon V, McNeely HE, Seminowicz D, Hamani C, et al. Deep Brain Stimulation for Treatment-Resistant Depression. Neuron 2005;45:651–60. https://doi.org/10.1016/j.neuron.2005.02.014.

[8] Malone DA, Dougherty DD, Rezai AR, Carpenter LL, Friehs GM, Eskandar EN, et al. Deep Brain Stimulation of the Ventral Capsule/Ventral Striatum for Treatment-Resistant Depression. Biol Psychiatry 2009;65:267–75. https://doi.org/10.1016/j.biopsych.2008.08.029.

[9] Schlaepfer TE, Bewernick BH, Kayser S, Mädler B, Coenen VA. Rapid Effects of Deep Brain Stimulation for Treatment-Resistant Major Depression. Biol Psychiatry 2013;73:1204–12. https://doi.org/10.1016/j.biopsych.2013.01.034.

[10] Neumann W-J, Huebl J, Brücke C, Gabriëls L, Bajbouj M, Merkl A, et al. Different patterns of local field potentials from limbic DBS targets in patients with major depressive and obsessive compulsive disorder. Mol Psychiatry 2014;19:1186–92. https://doi.org/10.1038/mp.2014.2.

[11] Bergfeld IO, Mantione M, Hoogendoorn MLC, Ruhe HG, Notten P, van Laarhoven J, et al. Deep Brain Stimulation of the Ventral Anterior Limb of the Internal Capsule for Treatment-Resistant Depression A Randomized Clinical Trial. Jama Psychiatry 2016;73:456–64. https://doi.org/10.1001/jamapsychiatry.2016.0152.

[12] Dougherty DD, Rezai AR, Carpenter LL, Howland RH, Bhati MT, O'Reardon JP, et al. A Randomized Sham-Controlled Trial of Deep Brain Stimulation of the Ventral Capsule/Ventral Striatum for Chronic Treatment-Resistant Depression. Biol Psychiatry 2015;78:240–8. https://doi.org/10.1016/j.biopsych.2014.11.023.

[13] Holtzheimer PE, Husain MM, Lisanby SH, Taylor SF, Whitworth LA, McClintock S, et al. Subcallosal cingulate deep brain stimulation for treatment-resistant depression: a multisite, randomised, sham-controlled trial. Lancet Psychiatry 2017;4:839–49. https://doi.org/10.1016/S2215-0366(17)30371-1.

[14] Coenen VA, Bewernick BH, Kayser S, Kilian H, Boström J, Greschus S, et al. Superolateral medial forebrain bundle deep brain stimulation in major depression: a gateway trial. Neuropsychopharmacology 2019;44:1224–32. https://doi.org/10.1038/s41386-019-0369-9.

[15] Raymaekers S, Luyten L, Bervoets C, Gabriëls L, Nuttin B. Deep brain stimulation for treatment-resistant major depressive disorder: a comparison of two targets and long-term follow-up. Transl Psychiatry 2017;7:e1251–e1251. https://doi.org/10.1038/tp.2017.66.

[16] Guidetti M, Marceglia S, Loh A, Harmsen IE, Meoni S, Foffani G, et al. Clinical perspectives of adaptive deep brain stimulation. Brain Stimulat 2021;14:1238–47. https://doi.org/10.1016/j.brs.2021.07.063.

[17] Scangos KW, Khambhati AN, Daly PM, Makhoul GS, Sugrue LP, Zamanian H, et al. Closed-loop neuromodulation in an individual with treatment-resistant depression. Nat Med 2021;27:1696–700. https://doi.org/10.1038/s41591-021-01480-w.

[18] Hu H, Cui Y, Yang Y. Circuits and functions of the lateral habenula in health and in disease. Nat Rev Neurosci 2020;21:277–95. https://doi.org/10.1038/s41583-020-0292-4.

[19] Roman E, Weininger J, Lim B, Roman M, Barry D, Tierney P, et al. Untangling the dorsal diencephalic conduction system: a review of structure and function of the stria medullaris, habenula and fasciculus retroflexus. Brain Struct Funct 2020;225:1437–58. https://doi.org/10.1007/s00429-020-02069-8.

[20] Dai D, Li W, Chen A, Gao X-F, Xiong L. Lateral Habenula and Its Potential Roles in Pain and Related Behaviors. ACS Chem Neurosci 2022;13:1108–18. https://doi.org/10.1021/acschemneuro.2c00067.

[21] Cui Y, Yang Y, Dong Y, Hu H. Decoding Depression: Insights from Glial and Ketamine Regulation of Neuronal Burst Firing in Lateral Habenula. Cold Spring Harb Symp Quant Biol 2018;83:141–50. https://doi.org/10.1101/sqb.2018.83.036871.

[22] Cui Y, Yang Y, Ni Z, Dong Y, Cai G, Foncelle A, et al. Astroglial Kir4.1 in the lateral habenula drives neuronal bursts in depression. Nature 2018;554:323–7. https://doi.org/10.1038/nature25752.

[23] Sartorius A, Kiening KL, Kirsch P, Gall CC von, Haberkorn U, Unterberg AW, et al. Remission of Major Depression Under Deep Brain Stimulation of the Lateral Habenula in a Therapy-Refractory Patient. Biol Psychiatry 2010;67:e9–11. https://doi.org/10.1016/j.biopsych.2009.08.027.

[24] Wang Z, Cai X, Qiu R, Yao C, Tian Y, Gong C, et al. Case Report: Lateral Habenula Deep Brain Stimulation for Treatment-Resistant Depression. Front Psychiatry 2021;11. https://doi.org/10.3389/fpsyt.2020.616501.

[25] Kiening K, Sartorius A. A new translational target for deep brain stimulation to treat depression. EMBO Mol Med 2013;5:1151–3. https://doi.org/10.1002/emmm.201302947.

[26] Zhang C, Kim S-G, Li D, Zhang Y, Li Y, Husch A, et al. Habenula deep brain stimulation for refractory bipolar disorder. Brain Stimulat 2019;12:1298–300. https://doi.org/10.1016/j.brs.2019.05.010.

[27] Zhang C, Zhang Y, Luo H, Xu X, Yuan T, Li D, et al. Bilateral Habenula deep brain stimulation for treatment-resistant depression: clinical findings and electrophysiological features. Transl Psychiatry 2022;12:52. https://doi.org/10.1038/s41398-022-01818-z.

[28] Wang Z, Jiang C, Guan L, Zhao L, Fan T, Wang J, et al. Deep brain stimulation of habenula reduces depressive symptoms and modulates brain activities in treatment-resistant depression. Nat Ment Health 2024. https://doi.org/10.1038/s44220-024-00286-2.

[29] Vissani M, Isaias IU, Mazzoni A. Deep brain stimulation: a review of the open neural engineering challenges. J Neural Eng 2020;17:051002. https://doi.org/10.1088/1741-2552/abb581.

[30] Priori A, Maiorana N, Dini M, Guidetti M, Marceglia S, Ferrucci R. Chapter Six - Adaptive deep brain stimulation (aDBS). In: Moro E, Polosan M, Hamani C, editors. Int Rev Neurobiol, vol. 159, Academic Press; 2021, p. 111–27. https://doi.org/10.1016/bs.irn.2021.06.006.

[31] Alagapan S, Choi KS, Heisig S, Riva-Posse P, Crowell A, Tiruvadi V, et al. Cingulate dynamics track depression recovery with deep brain stimulation. Nature 2023:1–9. https://doi.org/10.1038/s41586-023-06541-3.

[32] Frank AC, Scangos KW, Larson PS, Norbu T, Lee AT, Lee AM. Identification of a personalized intracranial biomarker of depression and response to DBS therapy. Brain Stimulat 2021;14:1002–4. https://doi.org/10.1016/j.brs.2021.06.009.

[33] Sonkusare S, Ding Q, Zhang Y, Wang L, Gong H, Mandali A, et al. Power signatures of habenular neuronal signals in patients with bipolar or unipolar depressive disorders correlate with their disease severity. Transl Psychiatry 2022;12:1–9. https://doi.org/10.1038/s41398-022-01830-3.

[34] Cobb BS, Coryell WH, Cavanaugh J, Keller M, Solomon DA, Endicott J, et al. Seasonal variation of depressive symptoms in unipolar major depressive disorder. Compr Psychiatry 2014;55:1891–9. https://doi.org/10.1016/j.comppsych.2014.07.021.

[35] Panaite V, Rottenberg J, Bylsma LM. Daily Affective Dynamics Predict Depression Symptom Trajectories Among Adults with Major and Minor Depression. Affect Sci 2020;1:186–98. https://doi.org/10.1007/s42761-020-00014-w.

[36] Kennedy SH, Giacobbe P, Rizvi SJ, Placenza FM, Nishikawa Y, Mayberg HS, et al. Deep Brain Stimulation for Treatment-Resistant Depression: Follow-Up After 3 to 6 Years. Am J Psychiatry 2011;168:502–10. https://doi.org/10.1176/appi.ajp.2010.10081187.

[37] Bewernick BH, Kayser S, Sturm V, Schlaepfer TE. Long-Term Effects of Nucleus Accumbens Deep Brain Stimulation in Treatment-Resistant Depression: Evidence for Sustained Efficacy. Neuropsychopharmacology 2012;37:1975–85. https://doi.org/10.1038/npp.2012.44.

[38] Crowell AL, Riva-Posse P, Holtzheimer PE, Garlow SJ, Kelley ME, Gross RE, et al. Long-Term Outcomes of Subcallosal Cingulate Deep Brain Stimulation for Treatment-Resistant Depression. Am J Psychiatry 2019;176:949–56. https://doi.org/10.1176/appi.ajp.2019.18121427.

[39] Peeters F, Berkhof J, Delespaul P, Rottenberg J, Nicolson NA. Diurnal mood variation in major depressive disorder. Emotion 2006;6:383–91. https://doi.org/10.1037/1528-3542.6.3.383.

[40] Wirz-Justice A. Diurnal variation of depressive symptoms. Dialogues Clin Neurosci 2008;10:337–43. https://doi.org/10.31887/DCNS.2008.10.3/awjustice.

[41] Scangos KW, Makhoul GS, Sugrue LP, Chang EF, Krystal AD. State-dependent responses to intracranial brain stimulation in a patient with depression. Nat Med 2021;27:229–31. https://doi.org/10.1038/s41591-020-01175-8.

[42] Bewernick BH, Kayser S, Gippert SM, Coenen VA, Schlaepfer TE. Acute antidepressant effects of deep brain stimulation – Review and data from slMFB-stimulation. Pers Med Psychiatry 2017;3:1–7. https://doi.org/10.1016/j.pmip.2017.01.002.

[43] Xiao J, Provenza NR, Asfouri J, Myers J, Mathura RK, Metzger B, et al. Decoding Depression Severity From Intracranial Neural Activity. Biol Psychiatry 2023;94:445–53. https://doi.org/10.1016/j.biopsych.2023.01.020.

[44] Sani OG, Yang Y, Lee MB, Dawes HE, Chang EF, Shanechi MM. Mood variations decoded from multi-site intracranial human brain activity. Nat Biotechnol 2018;36:954–61. https://doi.org/10.1038/nbt.4200.

[45] Kirkby LA, Luongo FJ, Lee MB, Nahum M, Vleet TMV, Rao VR, et al. An Amygdala-Hippocampus Subnetwork that Encodes Variation in Human Mood. Cell 2018;175:1688-1700.e14. https://doi.org/10.1016/j.cell.2018.10.005.

[46] Ashkan K, Rogers P, Bergman H, Ughratdar I. Insights into the mechanisms of deep brain stimulation. Nat Rev Neurol 2017;13:548–54. https://doi.org/10.1038/nrneurol.2017.105.

[47] Ramasubbu R, Lang S, Kiss ZHT. Dosing of Electrical Parameters in Deep Brain Stimulation (DBS) for Intractable Depression: A Review of Clinical Studies. Front Psychiatry 2018;9. https://doi.org/10.3389/fpsyt.2018.00302.

[48] Yeung AWK, Wong NSM. The Historical Roots of Visual Analog Scale in Psychology as Revealed by Reference Publication Year Spectroscopy. Front Hum Neurosci 2019;13. https://doi.org/10.3389/fnhum.2019.00086.

[49] Schiratti J-B, Le Douget J-E, Le van Quyen M, Essid S, Gramfort A. An ensemble learning approach to detect epileptic seizures from long intracranial EEG recordings. ICASSP 2018 - 2018 IEEE Int. Conf. Acoust. Speech Signal Process. ICASSP, Calgary, Canada: IEEE; 2018. https://doi.org/10.1109/ICASSP.2018.8461489.

[50] Banville H, Wood SUN, Aimone C, Engemann D-A, Gramfort A. Robust learning from corrupted EEG with dynamic spatial filtering. NeuroImage 2022;251:118994. https://doi.org/10.1016/j.neuroimage.2022.118994.

[51] Engemann DA, Mellot A, Höchenberger R, Banville H, Sabbagh D, Gemein L, et al. A reusable benchmark of brain-age prediction from M/EEG resting-state signals. NeuroImage 2022;262:119521. https://doi.org/10.1016/j.neuroimage.2022.119521.

[52] Giorgino T. Computing and Visualizing Dynamic Time Warping Alignments in R: The dtw Package. J Stat Softw 2009;31:1–24. https://doi.org/10.18637/jss.v031.i07.

[53] Sakoe H, Chiba S. Dynamic programming algorithm optimization for spoken word recognition. IEEE Trans Acoust Speech Signal Process 1978;26:43–9. https://doi.org/10.1109/TASSP.1978.1163055.

[54] Knowland D, Lim BK. Circuit-based frameworks of depressive behaviors: The role of reward circuitry and beyond. Pharmacol Biochem Behav 2018;174:42–52. https://doi.org/10.1016/j.pbb.2017.12.010.

[55] Kalin NH. The Critical Relationship Between Anxiety and Depression. Am J Psychiatry 2020;177:365–7. https://doi.org/10.1176/appi.ajp.2020.20030305.

[56] Sampogna G, Toni C, Catapano P, Rocca BD, Di Vincenzo M, Luciano M, et al. New trends in personalized treatment of depression. Curr Opin Psychiatry 2024;37:3. https://doi.org/10.1097/YCO.0000000000000903.

[57] Wei M, Qin J, Yan R, Li H, Yao Z, Lu Q. Identifying major depressive disorder using Hurst exponent of resting-state brain networks. Psychiatry Res Neuroimaging 2013;214:306–12. https://doi.org/10.1016/j.pscychresns.2013.09.008.

[58] Liu Y, Postupna N, Falkenberg J, Anderson ME. High frequency deep brain stimulation: What are the therapeutic mechanisms? Neurosci Biobehav Rev 2008;32:343–51. https://doi.org/10.1016/j.neubiorev.2006.10.007.

[59] Sani S, Busnello J, Kochanski R, Cohen Y, Gibbons RD. High-frequency measurement of depressive severity in a patient treated for severe treatment-resistant depression with deep-brain stimulation. Transl Psychiatry 2017;7:e1207–e1207. https://doi.org/10.1038/tp.2017.145.

[60] McIntyre CC, Anderson RW. Deep brain stimulation mechanisms: the control of network activity via neurochemistry modulation. J Neurochem 2016;139:338–45. https://doi.org/10.1111/jnc.13649.

[61] Iturrate I, Pereira M, Millán J del R. Closed-loop electrical neurostimulation: Challenges and opportunities. Curr Opin Biomed Eng 2018;8:28–37. https://doi.org/10.1016/j.cobme.2018.09.007.

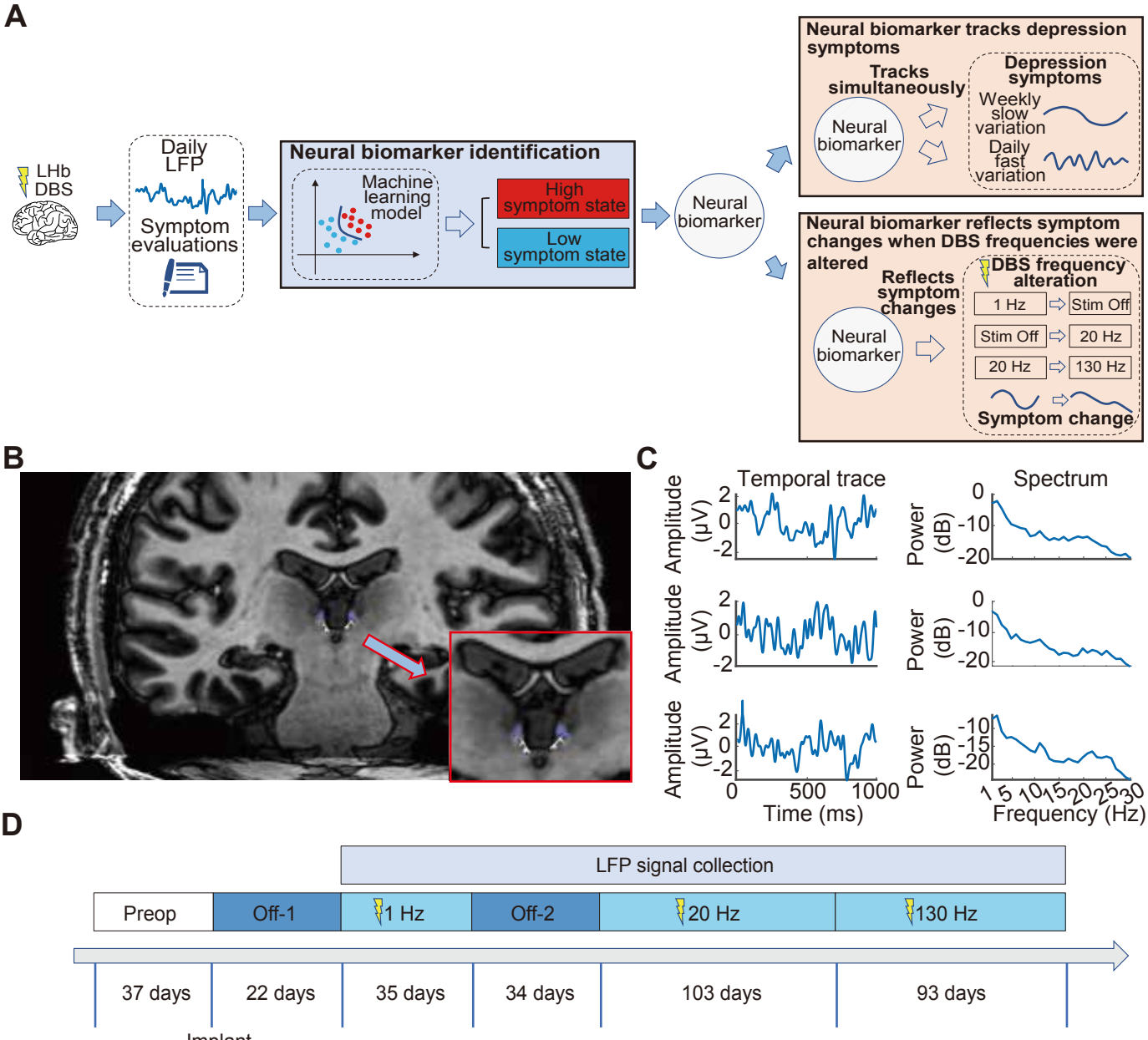
A
LHb
DBS
Daily
LFP
Symptom
evaluations
Neural biomarker identification
Machine
learning
model
High
symptom state
Low
symptom state
Neural
biomarker
Neural biomarker tracks depression
symptoms
Tracks
simultaneously
Neural
biomarker
Depression
symptoms
Weekly
slow
variation
Daily
fast
variation
Neural biomarker reflects symptom
changes when DBS frequencies were
altered
Reflects
symptom
changes
Neural
biomarker
DBS frequency
alteration
1 Hz
Stim Off
Stim Off
20 Hz
20 Hz
130 Hz
Symptom change
B
C
Temporal trace
Spectrum
Amplitude
(μV)
Power
(dB)
Time (ms)
Frequency (Hz)
D
LFP signal collection
Preop
Off-1
1 Hz
Off-2
20 Hz
130 Hz
37 days
22 days
35 days
34 days
103 days
93 days
Implant

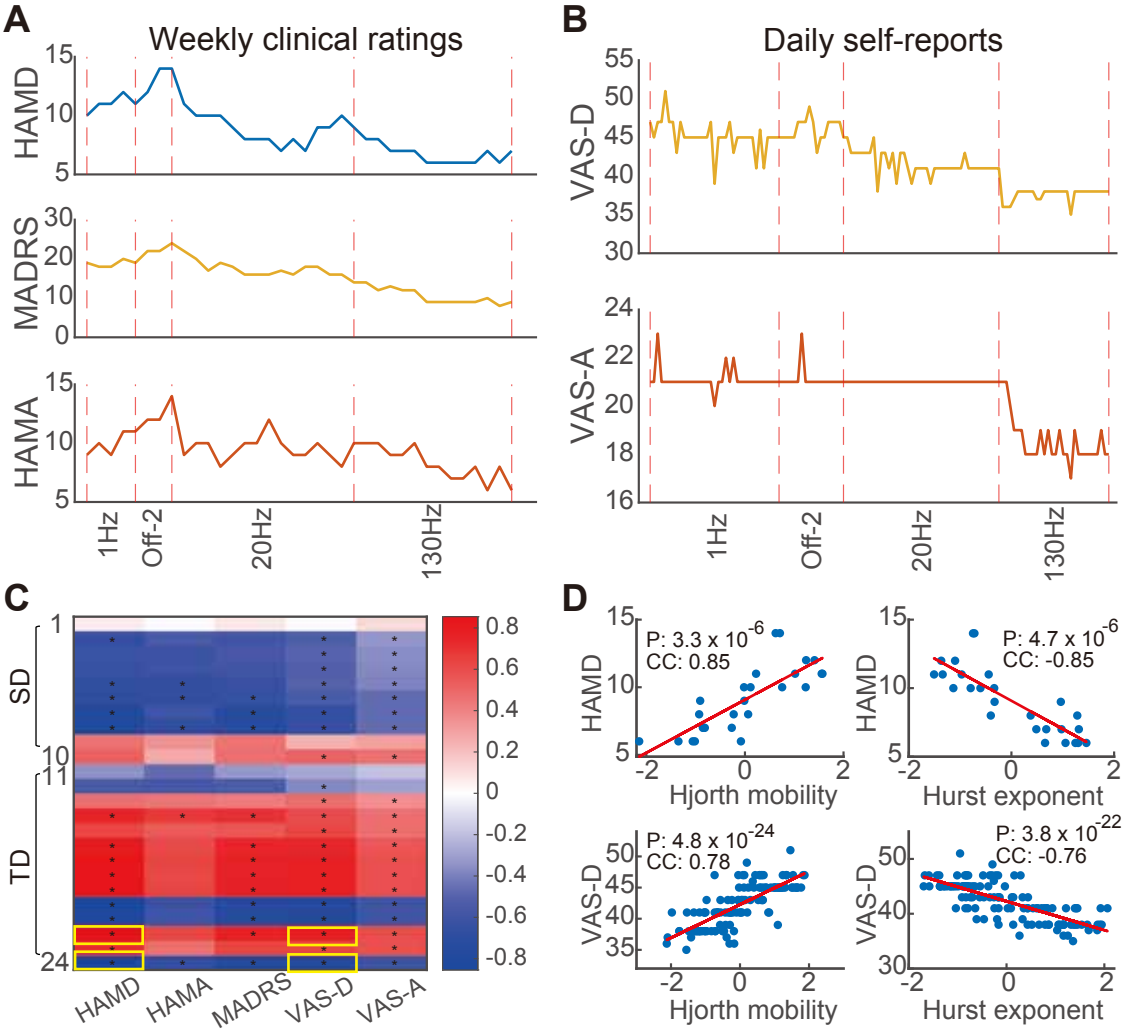
A
Weekly clinical ratings
HAMD
MADRS
HAMA
1Hz
Off-2
20Hz
130Hz
B
Daily self-reports
VAS-D
VAS-A
1Hz
Off-2
20Hz
130Hz
C
SD
TD
HAMD
HAMA
MADRS
VAS-D
VAS-A
D
P: 3.3 x 10^-6
CC: 0.85
HAMD
Hjorth mobility
P: 4.7 x 10^-6
CC: -0.85
HAMD
Hurst exponent
P: 4.8 x 10^-24
CC: 0.78
VAS-D
Hjorth mobility
P: 3.8 x 10^-22
CC: -0.76
VAS-D
Hurst exponent

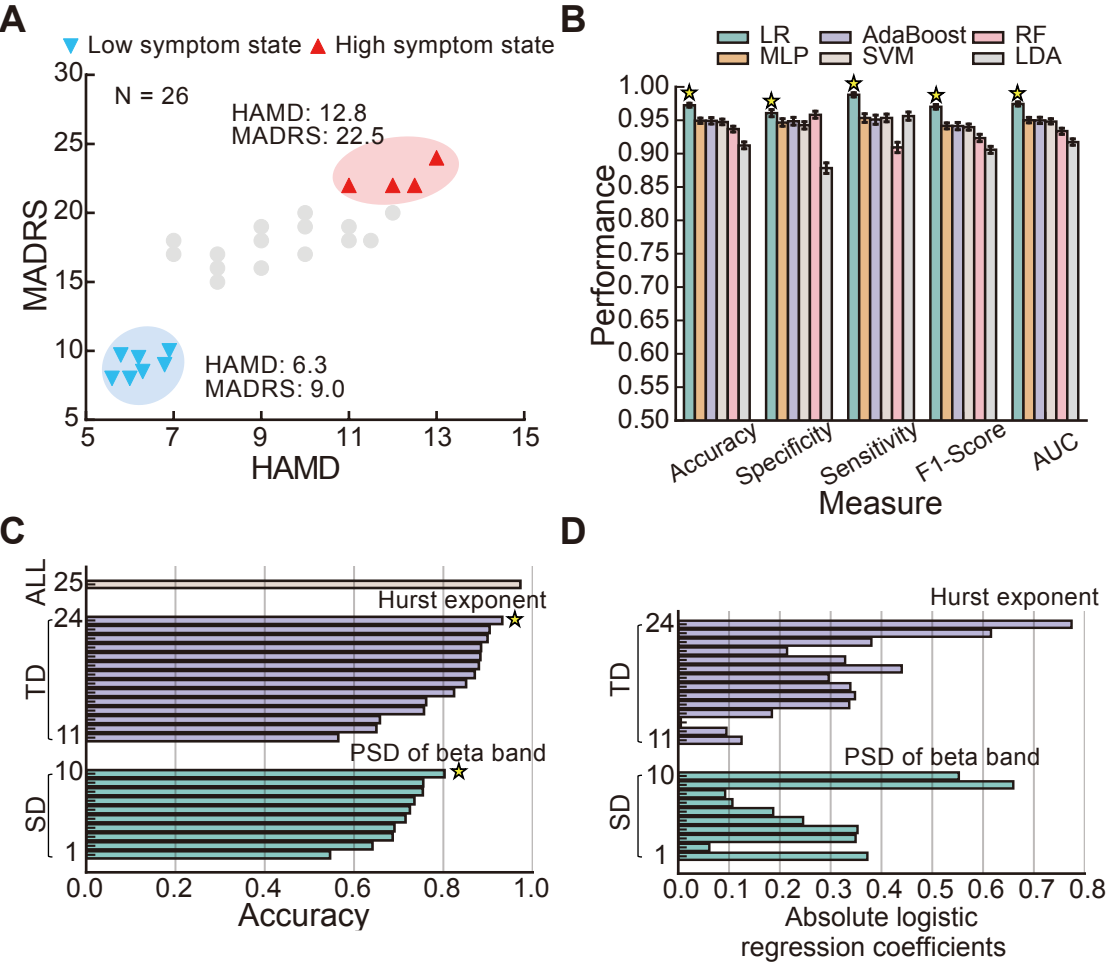
A
Low symptom state
High symptom state
N = 26
HAMD: 12.8
MADRS: 22.5
HAMD: 6.3
MADRS: 9.0
MADRS
HAMD
B
LR
MLP
AdaBoost
SVM
RF
LDA
Performance
Accuracy
Specificity
Sensitivity
F1-Score
AUC
Measure
C
ALL
TD
SD
Hurst exponent
PSD of beta band
Accuracy
D
Hurst exponent
PSD of beta band
Absolute logistic regression coefficients

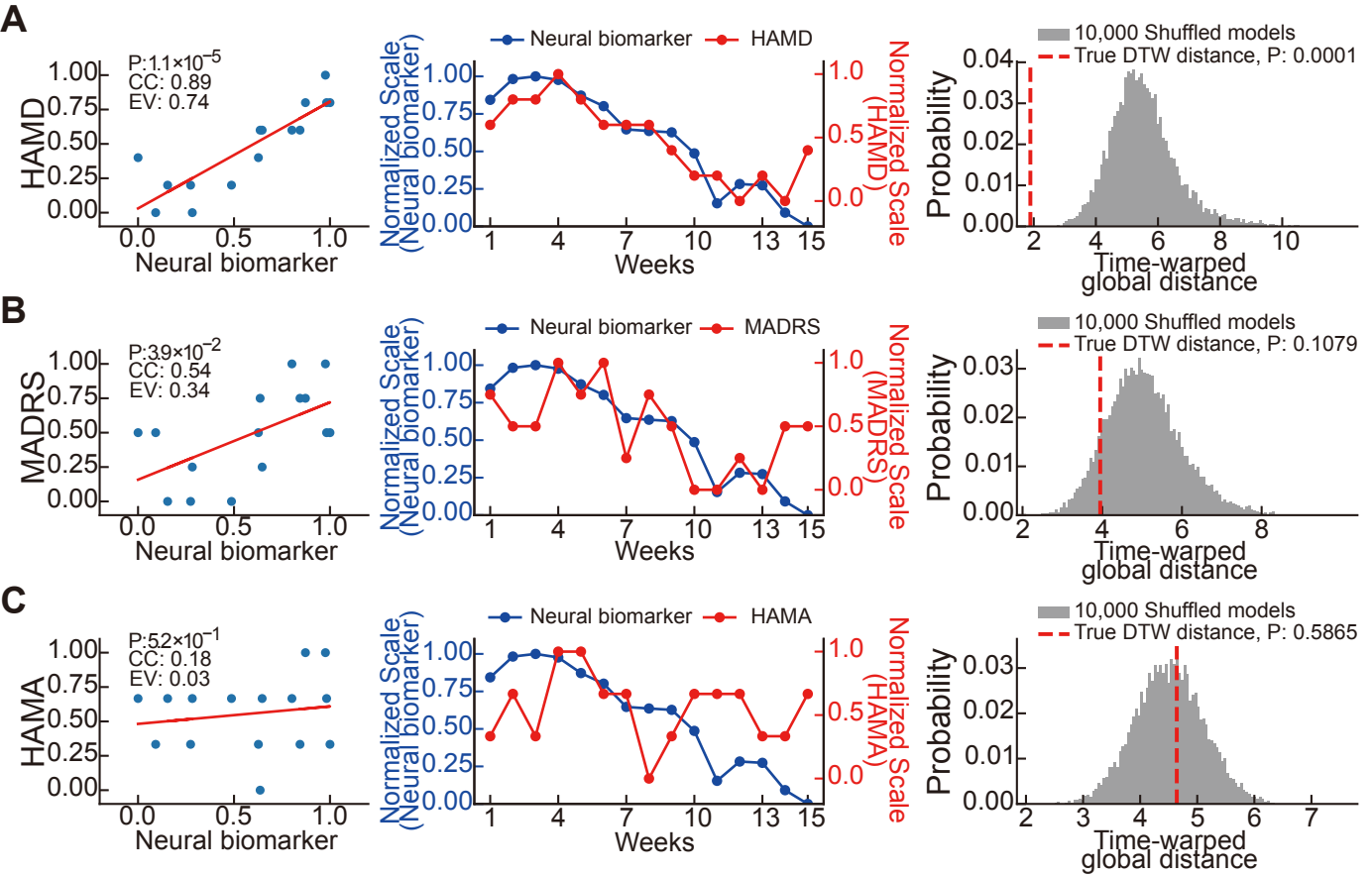
A
P:1.1×10−5
CC: 0.89
EV: 0.74
HAMD
Neural biomarker
Neural biomarker
HAMD
Normalized Scale (Neural biomarker)
Normalized Scale (HAMD)
Weeks
10,000 Shuffled models
True DTW distance, P: 0.0001
Probability
Time-warped global distance
B
P:3.9×10−2
CC: 0.54
EV: 0.34
MADRS
Neural biomarker
Neural biomarker
MADRS
Normalized Scale (Neural biomarker)
Normalized Scale (MADRS)
Weeks
10,000 Shuffled models
True DTW distance, P: 0.1079
Probability
Time-warped global distance
C
P:5.2×10−1
CC: 0.18
EV: 0.03
HAMA
Neural biomarker
Neural biomarker
HAMA
Normalized Scale (Neural biomarker)
Normalized Scale (HAMA)
Weeks
10,000 Shuffled models
True DTW distance, P: 0.5865
Probability
Time-warped global distance

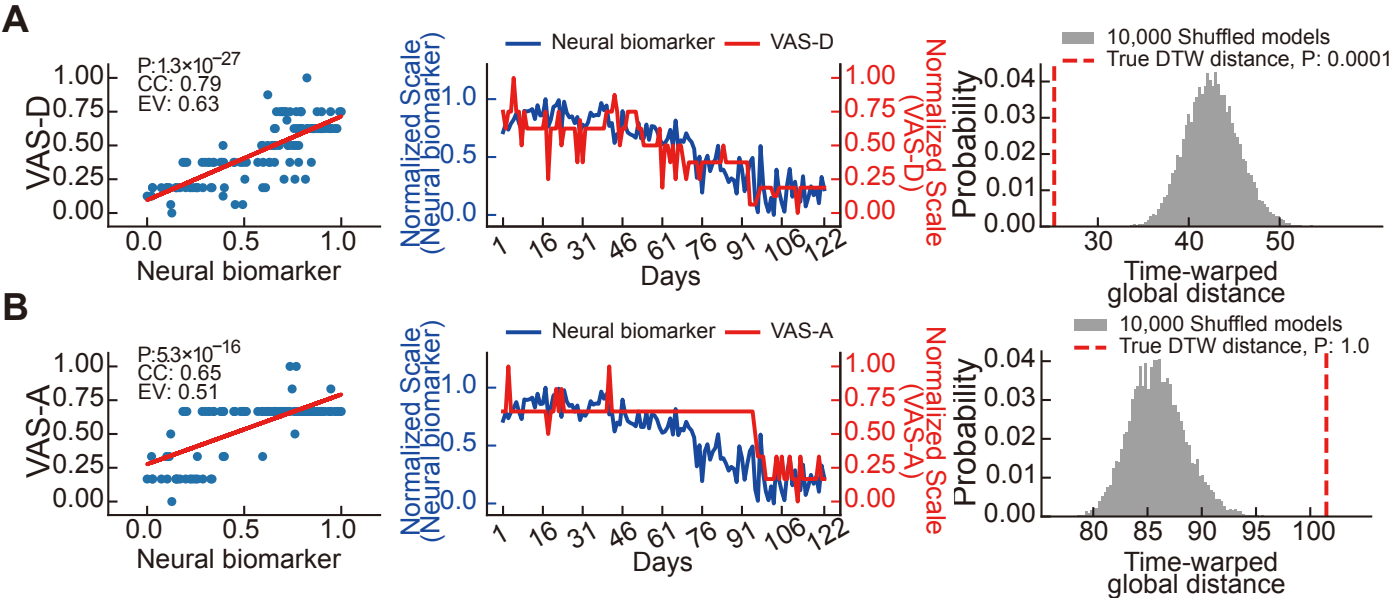
A
P:1.3×10^-27
CC: 0.79
EV: 0.63
VAS-D
Neural biomarker
Neural biomarker
VAS-D
Normalized Scale (Neural biomarker)
Normalized Scale (VAS-D)
Days
10,000 Shuffled models
True DTW distance, P: 0.0001
Probability
Time-warped global distance
B
P:5.3×10^-16
CC: 0.65
EV: 0.51
VAS-A
Neural biomarker
Neural biomarker
VAS-A
Normalized Scale (Neural biomarker)
Normalized Scale (VAS-A)
Days
10,000 Shuffled models
True DTW distance, P: 1.0
Probability
Time-warped global distance

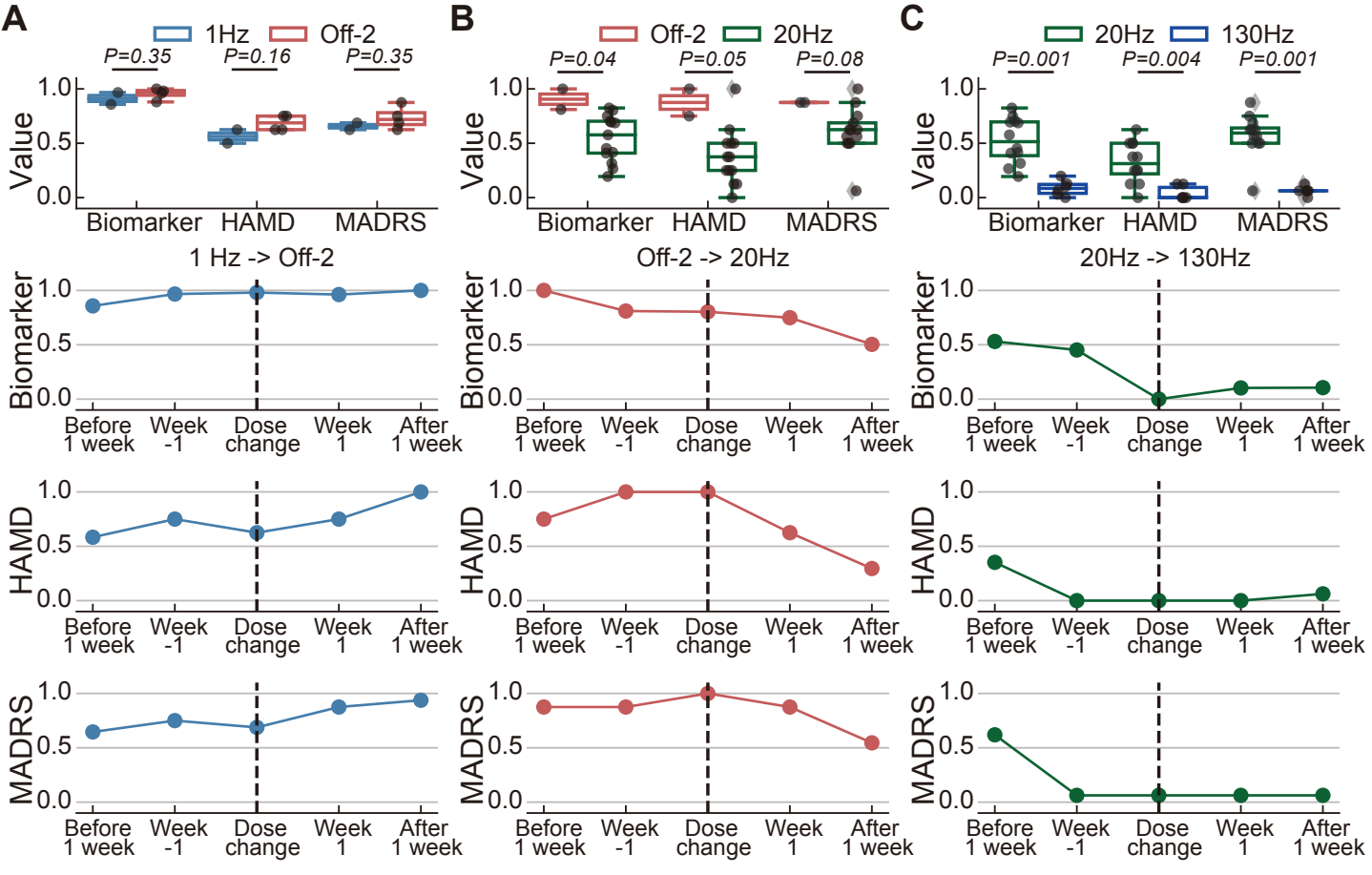
A
1Hz
Off-2
P=0.35
P=0.16
P=0.35
Value
1.0
0.5
0.0
Biomarker
HAMD
MADRS
1 Hz -> Off-2
B
Off-2
20Hz
P=0.04
P=0.05
P=0.08
Off-2 -> 20Hz
C
20Hz
130Hz
P=0.001
P=0.004
P=0.001
20Hz -> 130Hz
Before 1 week
Week -1
Dose change
Week 1
After 1 week